Published in final edited form as:
Cell Calcium. 2013 April ; 53(4): 264–274. doi:10.1016/j.ceca.2012.12.007.

Mechanical Regulation of Native and the Recombinant Calcium Channel

Angelo O. Rosa, **Naohiro Yamaguchi**, and **Martin Morad***
Cardiac Signaling Center, Medical University of South Carolina, University of South Carolina and Clemson University and Department of Regenerative Medicine and Cell Biology, Medical University of South Carolina, Charleston, South Carolina 29425

Abstract

L-type calcium channels are modulated by a host of mechanisms that include voltage, calcium ions (Ca^{2+} dependent inactivation and facilitation), cytosolic proteins (CAM, CAMKII, PKA, PKC, etc), and oxygen radicals. Here we describe yet another Ca^{2+} channel regulatory mechanism that is induced by pressure-flow (PF) forces of ~25 dyn/cm^2 producing 35–60% inhibition of channel current. Only brief periods (300ms) of such PF pulses were required to suppress reversibly the current. Recombinant Ca^{2+} channels (α1c77/β2a/α2δ and α1c77/β1/α2δ), expressed in HEK293 cells, were similarly suppressed by PF pulses. To examine whether Ca^{2+} released by PF pulses triggered from different sub-cellular compartments (SR, ER, mitochondria) underlies the inhibitory effect of PF on the channel current, pharmacological agents and ionic substitutions were employed to probe this possibility. No significant difference in effectiveness of PF pulses to suppress I_{Ca} or I_{Ba}, (used to inhibit CICR), was found between control cells and those exposed to U73122 and 2-APB (PLC and IP3R pathway modulators), thapsigargin and BAPTA (SERCA2a modulator), dinitrophenol, FCCP and Ru360 (mitochondrial inhibitors), L-NAMME (NOS inhibitor signaling), cAMP and Pertussis toxin (G_i protein modulator). We concluded that the rapid and reversible modulation of the Ca^{2+} channel by PF pulses is independent of intracellular release of Ca^{2+} and Ca^{2+} dependent inactivation of the channel and may represent direct mechanical regulatory effect on the channel protein in addition to previously reported Ca^{2+}-release or entry dependent mechanism.

INTRODUCTION

It has long been recognized that mechano-electrical feedback (MEF) plays a significant regulatory role in the physiology of the heart and pathophysiology of aortic stenosis [1], hypertension [2], cardiac failure [3], dilated cardiomyopathy [4] and sudden death [5].

Perhaps, the best known example of mechanical modulation of heart-function is the Frank-Starling law of the heart, which states that “Within physiological limits, the larger the volume of the heart, the greater are the energy of its contraction and the amount of chemical change at each contraction” [6, 7]. More recent studies have shown that immediately after cardiomyocyte stretch, action potential shortens, decreasing slightly the accompanying Ca^{2+}

*Correspondence: Address for correspondence: Prof. Martin Morad, Ph.D., Cardiac Signaling Center, 68 President Street, Charleston, BEB 321, SC 29425. moradm@musc.edu.

transient [8], despite the potentiated contraction. The increase in contraction was attributed to increased affinity of myofilaments to Ca^{2+} rather than an increase in intracellular Ca^{2+} [8, 9], but other possibilities that involve titin kinase [10], lattice spacing [11], troponin cooperativity [12] and changes in ryanodine receptor (RyR) open probability [13] have also been proposed. The shortening in action potential duration with stretch is thought to result either from suppression of the calcium current [7], or activation of non-selective or potassium-selective stretch channels [14].

More recently, pressurized fluid pulses were also shown not only to suppress Ca^{2+} currents in voltage clamped cardiomyocytes [15], but also to increase the frequency of Ca^{2+} sparks in cell periphery [16] and trigger calcium transients that originate from the mitochondria in intact myocytes [17].

The mechanisms by which pressure-flow (PF) pulses suppress Ca^{2+} channel currents remain still somewhat obscure. Though increased Ca^{2+} sensitivity of RyR or increased RyR leak has been suggested to contribute to the suppressive response [15, 18, 19], there appears to be significant diversity in the fluid pressure effect on L-type of calcium channels in different cell types (see table 1) [15, 20–25]. In smooth muscle cells, for instance, fluid pressure has enhancing, rather than suppressing effect on the channels [22, 26]. Other kinds of mechanical stimuli as positive patch pipette pressure, or hypotonic swelling also are reported to enhance L-type calcium channel current in smooth cells [22], although such effects appear to take place in a different time frame that are likely not to be compatible with a beat to beat modulation of calcium channels in heart cells.

Here we present data showing that fluid pressure accelerates the inactivation kinetics of Ba^{2+} transporting Ca^{2+} channel as it suppresses the channel under conditions where the cells were dialyzed by either low or high Ca^{2+}-buffered intracellular solutions. As PF-induced inactivation and blocking of Ba^{2+} currents were equally effective in low EGTA and high BAPTA dialyzing solutions and in cells additionally incubated in thapsigargin, it was unlikely that increased sensitivity of RyR to release Ca^{2+} was the underlying mechanism for mechanical sensitivity of the channel. Furthermore, we failed to detect any rise in cytosolic Ca^{2+} in voltage-clamped cells associated with pressure-flow pulse. Our data is more consistent with the idea that a direct mechanically activated intracellular pathway in addition to mechanically induced Ca^{2+} release mediates the effect of pressure-flow pulses on I_{Ca}.

METHODS

Cardiomyocytes Isolation

Cardiac myocytes were isolated from male Sprague Dawley rats (200–250 g, 7–10 weeks old) by established enzymatic cell isolation methods, as previously described [27]. Briefly, rats were deeply anaesthetized with sodium pentobarbital (150 mg kg^{-1} *i.p.*), and hearts rapidly excised in accordance with protocols approved by the Animal Care and Use Committees of the Medical University of South Carolina and University of South Carolina. The excised hearts were retrogradely perfused at 7 ml min^{-1} through the aorta, first with Ca^{2+}-free solution containing (mM): 137 NaCl, 5.4 potassium l-glutamate, 10 Hepes, 1 $MgCl_2$, 10 glucose, pH 7.3 at 37 °C, then with Ca2+-free solution containing Collagenase (1.4 mg ml^{-1}) and protease (0.16 mg ml^{-1}) for 15–22 min, and finally with a solution containing 0.2 mM $CaCl_2$ for 8 minutes. The tissue was then cut into several sections and gently agitated to dissociate the cells. The freshly dissociated cells were stored at room temperature in solutions containing 0.2 mM $CaCl_2$.

HEK293 cells cultures and transfection

The cDNAs of Ca^{2+} channel subunits α_{1C77}-YFP,β_1,$\alpha_2\delta$ were kind gifts of Dr. Nikolai Soldatov (NIA, Baltimore MD). The β_{2a} cDNA was kindly provided by Dr. Mark E. Anderson (University of Iowa, Iowa City, IA). HEK293 cells were grown in 6 well plates using DMEM, 10% FBS (Invitrogen) at 90% confluence and a penicillin 100 U/mL plus streptomycin 0.1mg/mL (Sigma). Using Lipofectamine™ 2000 (invitrogen) gene transfection assay, 1–6 μg of each subunit was mixed with a standard amount of lipofectamine reagent and incubated for about 20 minutes in serum and antibiotic free media. After incubation, the mixture was transferred to each well while swirling the plates. Cells were then incubated for 24 hours allowing for gene expression to take place, according to manufacturer instruction. The next day, cells were split on to coverslips at 10% confluence and allowed to incubate for another 48 hours before using them for patch clamp studies. Gene expression was visually confirmed to approximate 60–70% using a GFP fluorescence filter (CHROMA technology) for an excitement/emission range of 470/525nm. The GFP-filter was assembled onto the stage of a Nikon microscope and illuminated by a mercury arc lamp. Only cells expressing high green fluorescence levels were used for patch clamp experiments. The channels were expressed in HEK293 cells by using either α_{1C77}-YFP,β_1, $\alpha_2\delta$ or α_{1C77}-YFP,β_{2a}, $\alpha_2\delta$ combinations. Patch clamp experiments were done in K^+ and antibiotic free Tyrode's solution as described in Whole cell patch clamp section of methods.

Simultaneous measurements of Ca^{2+} transients and I_{Ca}

Single cardiomyocytes or transfected HEK293 cells were whole-cell clamped using pipette solutions containing in mM: 0.5 Fura-2 tetrapotassium salt, 120 CsCl, 20 TEA-Cl, 0.5 EGTA, 0.2 $CaCl_2$, 10 HEPES and 5 MgATP pH at (7.2) using CsOH. Osmalarity was corrected to 300 mOsm using CsCl. After a dialysis of 8–9 minutes, ratio-metric fluorescence of Fura-2 (F_{410} and F_{335}) was monitored using a 100W mercury arc lamp with an ellipsoidal reflector. The beam was split by a vibrating mirror, vibrating at 1150Hz, that served to multiplex the Ca^{2+}signal (OM, General Scanning, Watertown, MA, model IDS). One beam was reflected by an adjustable mirror and passed through an interference filter (410 nM), a dichroic mirror (DM_{370} long pass) and a field aperture before entering the microscope through the port used for epi-illumination. The other beam had the wavelength defined by an interference filter (335nm, 20nm band width) and it joined the first beam after being reflected through the dichroic mirror. Within the microscope the dichroic mirror (430nm) reflected the ultraviolet light toward the objective but transmitted the returning fluorescent green light toward the detection port. Most of the fluorescent light was transmitted through a beam splitter (BS) and an interference filter (IF510, 510 nm, 70 nm band width) and hit a photomultiplier (PM). The signal from the photomultiplier was de-multiplexed and yielded two signals corresponding to the two wavelengths of excitation (410nm and 335nm). A small part of the light was reflected by the beam splitter and was focused onto a TV camera that was connected to a monitor used in the alignment of the system. The patch clamp electrode was then placed over the cell, away from the illuminated segment, and a giga-seal was established. The adjustable aperture was now placed over the cell extending from its free end to the proximity of the electrode [28].

Whole cell patch clamp

Membrane currents were recorded in the whole-cell voltage-clamp configuration using a Dagan 3900A patch clamp amplifier (Dagan Corp., Minneapolis, MN), and a Digidata 1440A data acquisition system and pClamp 10 software (Axon Instruments/Molecular Devices, Sunnyvale, CA). Cell capacitance was calculated from the current transients to a 10 mV depolarizing pulse. The current signals were filtered at 10 kHz with a four-pole low-pass Bessel filter and digitized at 5–20 kHz before digitization and storage on a computer.

Currents were neither leak nor capacitance subtracted (to obtain high quality data and to control for myocyte viability), but the access resistance (1.5–3 times the pipette resistance) was compensated electronically to achieve a settling time constant of <0.5 ms. In parallel, P/N protocol was used to identify calcium channel activity, especially in HEK293 cells. The solution used for cellular equilibrium and formation of the gigaseal contained (mM): 137 NaCl, 5.4 KCl, 2 $CaCl_2$, 10 Hepes, 1 $MgCl_2$, 10 glucose, buffered to pH 7.4 with NaOH. Patch pipettes were filled with different solutions containing (mM): **1**, *Moderate-Ca^{2+} buffering* (2 EGTA, 1 Ca^{2+} 110 CsCl, 5 NaCl, 20 TEA-Cl, 10 Hepes, 5 Mg-ATP,). 2, *Super-Ca^{2+}-buffering* (10–20 BAPTA, 5 NaCl, 110 CsCl, 10 TEACl, 10 Glucose, 10 Hepes, 5 MgATP). 3, *Weak-Ca^{2+}-buffering* (0.2 EGTA, 110 CsCl, 5 NaCl, 20 TEA-Cl, 10 Hepes, 5 Mg-ATP). All solutions had their pH adjusted to 7.2 with CsOH and osmolarity adjusted to ~300mOsm using the predominant salt CsCl.

Following rupture of the membrane, myocytes were superfused with a Tyrode's solution that was devoid of K^+ to eliminate K^+ currents but contained either 2 mM Ca^{2+} or Ba^{2+} as the permeating ion through the Ca^{2+} channel. Ba^{2+} solutions were made using 0.5mM of EGTA to prevent Ca^{2+} presence in the external solutions. When used, drugs were dissolved in the external experimental solutions. Rapid (< 50 ms) changes in pressure were performed using an electronically controlled multi-barreled puffing system [29]. Puffing solutions heights were set at 28 cm or 6 cm above the experimental chamber, producing pressures heads of either 27,440 dyn/cm^2 or 5,883 dyn/cm^2 (using equation: $P = hg\rho$, where p is the pressure, h, height (28 cm), g, the acceleration of gravity (980 cm/s^2) and ρ = water density (1 g/cm^3)). Flow rate for the higher pressures (Q = 0.00436 cm^3/s) was calculated from Poiseuille's equation $[\pi r4(\Delta P)]/8\eta L$ where r = tube internal radius (0.014 cm), ΔP = pressure difference between the top and bottom of the tube (27,440 dyn/cm^2), η = fluid viscosity (0.01 poise), and L = tube length (9.5 cm). Dividing Q by cross-sectional area of the outflow tip (0.000 616 cm^2) gave a fluid velocity at the tip of 7.1 cm/s. Since (v/g) = t, where v = fluid velocity (7.1 cm/s), g = 980 cm/s^2 and t = time, the gravitational force would bring the fluid velocity to 7.1 cm/s in 7.25 ms. From $y = 1/2(gt^2)$, fluid would fall 0.257 mm due to gravity in 7.25 ms, hence the predicted pressure head at the outflow tip of the puffing device and therefore on the cell is 0.257 mmH2O. 0.257 mmH2O × [(9.81 N m–2)/1 mmH2O] × [1 dyn/cm^2/0.1 N/m^2] 25 dyn/cm^2. Multiplying Q (0.004 36 cm^3/s) by 60 s/min = 0.26 cm^3/min = 0.26 ml/min, which was experimentally verified by running solution through the tip for 1 min. (Figure 1). All experiments were carried out at room temperature (22–24 °C). Only cells with little leak current and clear edges were included in the final analysis of the results. Statistical comparisons were carried out using Student's *t* test. Differences were considered to be statistically significant to a level of $P < 0.05$. Numerical results are given as means ± S.E.M.

Voltage protocols

Cardiomyocytes were held at −50 mV to inactivate the Na^+ channels and Ca^{2+} or Ba^{2+} currents were activated by step depolarization to 0 mV; this protocol was applied at 0.1 or 0.2 Hz. Current-voltage (I–V) relations were constructed using depolarization pulses of −50 ms from a holding potential (HP) of 50 mV to 40mV, in 10mV increments. In some experiments I_{Ca} was measured using 50 ms long voltage ramps from holding potentials of −50mV to +80mV.

Time constant of inactivation for I_{Ca} or I_{Ba} were calculated using the formula:

$$f(t)=\sum_{i=1}^{n} A_i e^{-t/\tau i}+C$$

RESULTS

PF-pulses suppress and accelerate the inactivation kinetics of calcium channel

Figure 2 shows the effect of a single 500ms long PF pulse (pressure head, 28 cm of water) on the magnitude and time course of I_{ca}, recorded in a moderately Ca-buffered (dialyzed with 2 mM EGTA) ventricular myocyte and bathed in the same solution as that applied by the puffing pipette, before (Fig. 2D trace a), 500ms after application of the PF-pulse (trace b), and 60 s after termination of pressure-puff pulse (trace c). I_{Ca} was suppressed rapidly and reversibly (within ~20s) for PF pulses lasting 500ms. When I_{Ca} traces were normalized to their peaks values, the PF pulse effect in accelerating the inactivation kinetics of I_{Ca} was clearly apparent (Fig.2C) and was quantified in Fig.2B.

In the next set of experiments the effects of longer PF-pulses in weakly-Ca^{2+}-buffered myocytes (0.2 mM EGTA) was examined. Figure 3*A* shows, in open circles, I_{Ca} measured every 5s while the cell is subjected to continuous but very low pressure-flows of bathing solutions (pressure-head, 6 cm water). At such small PF forces, there was always a run-down of I_{Ca} within the 500s experimental periods. Fig 3 A (red traces) also shows the suppressive effects of larger PF-forces (28 cm of H_2O) on peak I_{Ca} applied for 150s (30 I_{Ca} episodes) before returning the PF-force back to control levels. This figure represents a set of 4 experiments in which we quantified the onset, the effectiveness, and the slow recovery from the PF-suppressive effects on Ca^{2+} channels. Figure 3A, inset traces, shows the details of the fast suppressive effects of higher PF-forces on I_{Ca} and its reversibility in a single representative myocyte. Note that the higher PF force suppresses peak I_{Ca} rapidly, but the current recovery occurs much slower, long after the PF-force is returned to control levels (6 cm H_2O). Fig. 3B quantifies I_{Ca} as the difference-current to eliminate the effect of current run-down.

PF-effect on Ba^{2+} transporting calcium Channels

Figure 4*A* shows the effect of a single 500ms long PF pulse (28 cm of water pressure head) on the magnitude and time course of I_{Ba}, recorded from a ventricular myocyte bathed in the same Ba^{2+}-containing solution as that applied by the puffing pipette, before (trace a), 500ms after application of the pulse (trace b), and 20 s after termination of fluid pulse (trace c). I_{Ba} was suppressed rapidly and reversibly (within ~5 s) for short applications of PF pulses. When I_{Ba} traces were normalized to their peaks values, the PF effect on the inactivation kinetics was clearly apparent (Fig.4B) and was quantified in Fig.4C. Although the degree of inactivation of I_{Ba} varied greatly in different animals, the suppressive effect was not accompanied by the same degree of acceleratedkinetics, suggesting either two independent mechanisms or a single two-tiered process. **Figure** 4*C* compares the time course of PF-induced suppression of I_{Ba} and the accompanying accelerated inactivation kinetics. Figure 4*D* represents the voltage-dependence of a PF blocked currents using a ramp pulse protocol applied from a holding potential of −50 to +80mV. The I–V relation of PF-suppressed current, determined using Cd^{2+} subtracted currents, was consistent with that recorded for L-type calcium channel current (activating at −30mV, peaking at ~zero mV, reversing at ~ 70 mV). In Cd^{2+} containing solutions there was no measurable PF-blocked current suggesting PF pulse was suppressing only the calcium channel currents.

Pressure-flow pulses suppress the human recombinant α1c77/β1/α2δ and α1c77/β2a/α2δ channels

In order to exclude other potential complicating factors, including possible PF-effects on other voltage gated channels we expressed all the subunits of L-type calcium channels in HEK293 cells using either β1 or β2a subunits and subjected such cells to PF-pulses. In these experiments, cells were submitted to 500ms of PF and test pulse was given after 200ms of

PF. There was a consistent and strong effect of PF on both the peak current-amplitude and the inactivation kinetics of I_{Ba} in the recombinant channels. Figure 5 shows that the magnitude of suppression varied significantly in different cells (compare current traces in Panel *A* to *B*, and panel *C* to *D*) independent of the subunits expressed. Cells expressing β_1 subunit had slightly faster inactivation kinetics than the β2a expressing cells, but the PF-induced acceleration of inactivation kinetics was remarkably similar in most of the cells independent of the level of block achieved (compare panels *A* to *B*, and panels *C* to *D* and the normalized traces in panel E). Figure 5F shows that the time constant of inactivation in β1 containing channels changed ~62% (from 342.0 ± 41.0 to 129.0 ± 28.0 ms (n=3)), while in β2a containing channels the change was about 52% (from 440.0 ± 21.0 to 207.5 ± 23.5 ms (n=3)). The PF-effects in recombinant human Ca^{2+} channels confirmed the findings described above for the rat ventricular myocytes suggesting that the PF-effects are specific to the channel itself.

PF-pulse duration determines the magnitude of the block and extent of inactivation

Figure 6 shows the degree of suppression of I_{Ba} in HEK293 cells in response to PF-pulses of different durations. In this set of experiments we used the α1c77/β2a/α2δ recombinant channel because the voltage dependent inactivation of I_{Ba} in this recombinant channel had been previously described to be very slow [30], allowing for the quantification of PF response using long depolarizing pulses. The duration of the PF-pulse was prolonged from 50 to 700 ms (PF bar, middle row traces A–D). Current traces activated at 5s intervals before, during, and after application of PF-pulses are shown in black. Grey traces represent the recording of the current prior to and 5 second following the application of PF-pulse. The results show that PF-pulses shorter than 50ms had little or no effect on I_{Ba} when applied during the depolarizing pulse or on the current activated 5 s later (compare black and gray traces in panel A). On the other hand, as the duration of the PF-pulse was increased to 100, 200, or 700ms, (Figure 6*B*, *C* and *D*) the magnitude of the PF-effect increased both during activation of I_{Ba} and on currents activated 5–10 seconds following the PF-pulse.

Mitochondrial calcium release in mediating the PF-effect on calcium channels

Since PF-pulses have been reported to induce a transient rise in cytosolic Ca^{2+}, originating from the mitochondrial calcium pools in non-dialyzed intact cells [17], we examined the possible role of mitochondrial calcium stores in mediating the PF-effects on calcium channels. We used well known pharmacological agents that inhibit mitochondrial function such as the protonophore FCCP (0.1–5μM, to depolarize mitochondrial membrane potential), mitochondrial calcium uniporter inhibitor, Ru360 (1μM), the mitochondrial sodium-calcium exchanger blocker, CGPP37157 (1–10μM), the mitochondrial uncoupler dinitrophenol (100μM) or 2h pre-incubation with the mitochondrial permeability transition pore inhibitor cyclosporine (0.5μM). The results of these extensive studies are summarized in Table 2, and suggest that although all of these compounds partly suppressed the calcium channel current, none modified the PF-induced suppression of I_{Ba} significantly.

PF-effects on I_{Ba} in highly Ca^{2+}-buffered and SERCA2-suppressed myocytes

In another series of experiments, the effects of PF-pulses on I_{Ba} were quantified in paired cells dialyzed with different concentrations of Ca^{2+} buffers in the same experimental day (Figure 7*A and B*). PF-pulses were found to be equally effective in suppressing the Ca^{2+} channel currents whether cells were dialyzed with 2 mM EGTA plus 1mM Ca^{2+} (~100nM free Ca^{2+}) or with 10mM BAPTA (no added Ca^{2+}). Generally the patched cells were dialyzed for 9 minutes with BAPTA before start of electrophysiological measurements. Even longer dialyzing periods, in excess of 30 minutes, failed to alter the PF-suppressive effects significantly.

In yet another set of experiments, 2 to 4 coverslips plated with cardiomyocytes were treated with SERCA2a inhibitor thapsigargin (1μM) for at least 30 min. To assure that SERCA2a and Ca^{2+}-release from the SR was inhibited we measured the rise of intracellular Ca^{2+} in response to depolarizing pulses from −50 to 0mV, or applications of 10mM caffeine. Neither of the procedures triggered measureable calcium release in Fura-2 dialyzed myocytes (data not shown). Once again, there were no significant differences in the PF-effect whether the cells were dialyzed with 2mM EGTA or 10mM BAPTA intracellular solutions. In the thapsigargin-treated batch of cells PF-pulses continued to suppress I_{Ba} to the same extent as the untreated cells. In a set of thapsigargin-incubated cells that were also dialyzed with thapsigargin (0.1–10μM) or thapsigargin plus caffeine (10mM) through the patch pipette to assure complete depletion of SR and ER stores, we found, once again, no significant alterations in the PF-induced response on $I_{Ba.}$ In addition, incubation of myocytes in 100 μM APB-2 (an IP-3 receptor blocker), plus its direct extracellular application also failed to alter the PF-induced suppression of I_{Ba} (Figure 8). The results, in sum, appear to exclude a significant role for ER or SR calcium release in the PF-induced suppression of I_{Ba}.

ER and mitochondrial inhibitors and the PF-induced suppression of I_{Ba}

In a group of myocytes that were incubated for 30 min in 1 μM thapsigargin we tested for the possible involvement of mitochondrial Ca^{2+} stores by using a host of pharmacological inhibitors of mitochondrial function that included uncoupler of electron transport (0.1 μM of FCCP or 100 μM dinitrophenol), mitochondrial Ca^{2+} uniporter blocker, (1 μM Ru360), mitochondrial NCX blocker, (10 μM CGP37157), or cytochrome c release blocker, (cyclosporine, 500nM).

No significant differences in PF-induced suppression of I_{Ca} were noticed between cells exposed to mitochondrial inhibitors compared to those treated only with thapsigargin (see table 2). It appears therefore, that simultaneous elimination of the two major calcium stores in the cells failed to change the PF-suppressive effect on calcium channel current.

Modulation of intracellular signaling pathways and the PF response

In order to evaluate the role of the major calcium channel modulatory pathways in the PF-efficacy, we tested the effectiveness of PF-induced I_{Ca} suppression under conditions where the states of phosphorylation, NOS-signaling, or the stretch-activate pathways were altered. cAMP (200 μM), PLC inhibitor U73122 (1μM), NOS inhibitor L-NAME (1mM), G-protein inhibitor pertussis toxin (0.1μM for 30 min), and Ca^{2+}-channel agonist Bay-k8644 (1μM), all failed to significantly alter the PF-effect on Ca^{2+}-channel currents (Table 2).

DISCUSSION

The major finding of this study is that pressurized fluid flow (PF) pulses suppress the calcium channel currents (Ca^{2+}, Ba^{2+}) independent of voltage, and calcium release from intracellular stores. Our data confirms a previous report by Lee et al [15], showing similar fast PF-induced suppression of I_{Ca}, but in contrast to those observations, our PF-effect appears not to require any known cellular sources of Ca^{2+} or modulation of Ca^{2+}-signaling mechanisms. The mechanical regulation of Ca^{2+} channel appears to have evolved along tissue functional demands as different subtype of L-type calcium channels expressed in different tissues respond differently, to mechanical forces (see Table 1, and [15, 20–25]. Our findings suggest that PF-effect does not depend exclusively on activation of CICR or cytosolic rise of Ca^{2+}, but it can regulate Ca^{2+} channel current independent of intracellular Ca^{2+}-release. This assertion is supported by the findings in HEK293 cell expression system, devoid of significant CICR, where a strong suppressive effect of PF on the recombinant human channels containing either beta-1 or beta-2a subunits was consistently observed. We

also found little evidence for significant involvement of mitochondrial or IP3-gated Ca^{2+}-stores because pharmacological inhibitors of these pathways and dialysis of such cells with very high BAPTA concentrations failed to modify the PF-induced suppression of the Ca^{2+} channel. These findings led us to conclude that PF-effects may occur independent of cellular calcium signaling pathways and, as such, may serve as a mechanically regulated mechanism in tandem with those requiring Ca^{2+}-release or entry.

PF-induced suppression of I_{Ba} in HEK293 cells

Suppression of I_{Ba} by PF-pulses, in HEK293 cells expressing α1c77/β2a/α2δ channels, had a latency of about 300ms. PF-pulses lasting 50ms to 100ms had no apparent effect on the first depolarization-pulse (pulse where PF were applied), but had a small effect on pulses given 5s later, inactivating $I_{Ba.}$ Longer pulses (200 to 700ms) inactivated the current not only during the time course of the same depolarizing pulse, but also continued to suppress the current generated 5s later. The finding that the PF-effect initiates rapidly, ~300ms (see current inactivation in middle pulses in Figure 6) is in agreement with the idea that a direct mechanical mediated the PF-effect. The data also implies that the channels may adapt steeply to pressure-flow forces, exhibiting both threshold and asymmetrical delays in its activation and recovery.

Even though β1-containing channel showed faster inactivation kinetics than β2- channels (299 ± 6.6 ms vs. 522 ± 22 ms, respectively), we found that channels expressing either one of these subunits have their inactivation kinetics modified by PF (130 ms and 115 ms, respectively). These findings suggest that suppression of calcium channel current and the acceleration of its kinetics is present regardless the β subunit expressed.

Does Ca^{2+} influx or release play a role in PF-induced effect?

Mechanical stimulation has been shown to produce Ca^{2+} increases in a variety of cell types including epithelia [31], cardiac and skeletal muscle [17, 32, 33], endothelial cells [34], glia [35], osteoblasts [36] and sensory neurons [37]. Also, it is generally accepted that Ba^{2+} transporting calcium channels are unable to trigger Ca^{2+} release from the SR and thereby activate CICR [38]. Nevertheless, since PF-induced suppression was equally effective on I_{Ba} and I_{Ca} (Figures.2, 3, 4 & 6), we tested whether other sources of Ca^{2+} release or entry were involved in mediating the PF response on I_{Ba}. To eliminate all sources of Ca^{2+} release or contaminating Ca^{2+}, the PF-effect on I_{Ba} was quantified under the following experimental conditions: 1) Myocytes incubated in thapsigargin and exposed to 10 mM of caffeine to rule out both ER and SR calcium stores; 2) myocytes incubated in thapsigargin were also dialyzed with thapsigargin plus 20 mM BAPTA; 3) Myocytes incubated in thapsigargin were exposed to Ba^{2+} containing zero Ca^{2+} solution plus 0.5mM EGTA to prevent contaminant extracellular sources of Ca^{2+}. 4) Myocytes incubated in thapsigargin were exposed also to a number of mitochondrial inhibitors (Dinitrophenol, FCCP, RU360). In the set of myocytes pre-treated with thapsigargin and exposed to any of the 4 conditions listed above, we found no significant differences in the PF effects as compared to non-treated cells, suggesting that Ca^{2+} release from the SR/ER, mitochondria, or entry of Ca^{2+} across the plasma membrane were not the dominant factors in the PF suppressive effect on I_{Ba}. In yet another set of experiments myocytes from the same thapsigargin-treated batch were subjected to global imaging of Ca^{2+} (fluorometric, or confocal) to directly probe for possible rises of cytosolic Ca^{2+}. We found no indication of rise in cytosolic Ca^{2+} accompanying the PF-effect on I_{Ba}. This set of finding is somewhat puzzling in the light of previously reported PF-induced mitochondrial Ca^{2+}-release in intact non-dialyzed myocytes [17] as well as the reported strech-induced increase in open probability of RyRs [19], but maybe reconcilled if both Ca^{2+}-dependent and –independent mechanism were present in the cardiomyocytes. Considering the variability of mechanical forces encountered by the myocyte (stretch,

pressure, flow, sheer, etc.), perhaps it is not surprising that variable regulatory Ca^{2+}-dependent and-independent mechanisms may have evolved to regulate the cardiac contractile force.

Since pre-exposure of cells to Bay-K8644 suppresses the calcium dependent inactivation (CDI), this drug may provide a good tool for evaluating the role of CDI in mediating the PF effect on I_{Ba} [39]. Even though we observed an increase in current amplitude ($I_{Ba,}$ I_{Ca}) and a pronounced decrease in CDI elicited by Bay-K8644 (I_{Ca}), we did not see any significant alteration in the PF effects on I_{Ca} or I_{Ba} (table 2), suggesting little or no role for CDI in mediating the PF-effect on I_{Ba}.

Mitochondrial Calcium and the PF effect

Others and we have shown that mitochondrial calcium release modulate cell signaling, modifying EC-coupling in cardiomyocytes [17] or calcium transients in other cell types [40]. Based on those findings we manipulated the mitochondrial Ca^{2+}-signaling pathways by exposing the myocytes to blockers of MCU, mitochondrial NCX and cytocrome c release. Some of these agents, namely the mitochondrial un-couplers [41], and mitochondrial NCX blocker [42] also suppressed the calcium current as have been previously noted. As shown here, we found that PF-induced block of L-type Ca^{2+} current does not require mitochondrial Ca^{2+} release. PF was previously shown to produce mitochondrial Ca^{2+} signaling in the intact cardiomyocytes [17]. It is possible that whole cell configuration used to clamp cardiomyocytes may cause loss of soluble factors required for PF-induced mitochondrial calcium release that would produce additional PF-induced inactivation and block of L-type Ca^{2+} channels. Nevertheless, in the present study we found mechanical effect of PF on L-type Ca^{2+} channels activities in the total absence of mitochondrial signaling. Thus, though all the mitochondrial inhibitors used in this study failed to alter the PF-effects on the amplitude or inactivation kinetics of calcium channel currents, supporting the idea that the PF-effect on calcium current is independent of calcium release, the data do not exclude the presence of Ca^{2+}-dependent mechanical regulatory mechanisms mediated by Ca^{2+}-release also from the mitochondria .

Possible role of other intracellular signaling pathways in mediating the PF- effect

Many intracellular signaling pathways that include PLC, PKA and G proteins signaling modulate calcium channel open probability or inactivation [43–48]. Mechanical stress, in the form of stretch, has been reported to activate phospholipase C and elevate intracellular calcium levels in neonatal rat cardiomyocytes [49]. This could theoretically be the mechanism that underlies the effect of pressurized flow force on I_{Ba} in our study. However, our results showed that inhibition of PLC did not change the inactivation or blocking of I_{Ba} induced by PF-pulses, implying that PF effect maybe somewhat different than the stretch effect on I_{Ca}. Increase of kinase activities with beta-adrenergic agonists, also known to modulate L-type Ca^{2+} channel and SERCA2 activities, [50, 51] also failed to significantly modify the effect of PF on I_{Ba} (Table 2). The Ca^{2+}-independent PF-effect on the Ca^{2+}-channel, therefore, appears not to require phosphorylation through either PKC or PKA pathways.

Nitric oxide has also been reported to inhibit the L-type Ca^{2+} current in rat ventricular myocytes via a G-protein signaling pathway [52]. The possibility that PF-effect was mediated through NO or G protein activation was probed using myocytes exposed to or dialyzed with both L-NAME or pertussis toxin. We could not indentify any measurable change in the effect of PF on I_{Ba} under such conditions.

Considering that inhibition or enhancement of a number of pathways mentioned above failed to show significant differences in the PF effect on I_{Ba}, the data appears to point towards a direct mechanical mechanism on the channel proteins.

Pathophysiological implications of PF effect

Although the PF-effect on I_{Ca} appeared somewhat less prominent than on I_{Ba}, and was more variable between animals, the effect in cells dialyzed with low-calcium buffered solutions (approximating the intact cells) was fast and reversible for both peak current and the inactivation parameters. Furthermore, in addition to the rapid PF responses there also was a maintained PF-effect that persisted for the duration of the PF perturbation, and reversed following the termination of PF-pulse (Fig. 3). This finding excludes the possibility that PF-effect is exclusively related to the extent of calcium buffering and suggests that this mechanical mechanism maybe physiologically relevant in regulating the channel function somewhat similar to voltage- or calcium-dependent inactivation and facilitation.

Since blood pressure and volume inside the heart chambers changes constantly with every beat, it is likely that such pressure forces modulate the cardiac calcium channels in the intact heart and thereby serves as a feedback mechanism for the regulation of the contractile force. Aortic stenosis or systemic hypertension might dampen such auto-regulatory mechanism and eventually contribute to events causing cardiac hypertrophy. In fact, decreased cardiac L-type Ca^{2+} channel activity has been associated with cardiac hypertrophy and failure in mice [53]. Since calcium channels directly regulate calcium entry into the myocytes thereby determining the strength of contraction and cardiac output, it is likely that feedback mechanisms related to pressure-flow forces, somewhat similar to our findings, may serve as dynamic cardiac regulatory mechanisms in the intact heart. Consistent with this idea, it has been reported that the Ca^{2+} channel open probability in chick embryonic ventricular myocytes decreases by disruptors and increases by stabilizers of cyto-skeletal proteins [54]. It is possible, therefore, that PF forces "*restructure*" the calcium channel assembly with cytoskeleton proteins, leading possibly to brief and reversible disassembly of the channel, as reflected by reduced current. Brief disturbances in such physical coupling may account for physiological regulation of I_{Ca} whereas maintained or pathological changes in pressure might irreversibly alter calcium channel activity leading to a host of cardiac pathologies.

Acknowledgments

We are grateful to Dr. Lars Cleemann and John Scaringi for their technical support and suggestions. Supported by NIH grants: R01-HL 16152, R01-HL107600 and R03-AR061030, AHA grant: 10SDG3500001, and NSF grant: EPS-0903795

References

1. von Olshausen K, Schwarz F, Apfelbach J, Rohrig N, Kramer B, Kubler W. Determinants of the incidence and severity of ventricular arrhythmias in aortic valve disease. Am J Cardiol. 1983; 51:1103–1109. [PubMed: 6837454]
2. Webb AJ, Rothwell PM. Blood pressure variability and risk of new-onset atrial fibrillation: a systematic review of randomized trials of antihypertensive drugs. Stroke. 2010; 41:2091–2093. [PubMed: 20651263]
3. Reiter MJ. Effects of mechano-electrical feedback: potential arrhythmogenic influence in patients with congestive heart failure. Cardiovasc Res. 1996; 32:44–51. [PubMed: 8776402]
4. Sarubbi B, Ducceschi V, Santangelo L, Iacono A. Arrhythmias in patients with mechanical ventricular dysfunction and myocardial stretch: role of mechano-electric feedback. Can J Cardiol. 1998; 14:245–252. [PubMed: 9520861]
5. Babuty D, Lab MJ. Mechanoelectric contributions to sudden cardiac death. Cardiovasc Res. 2001; 50:270–279. [PubMed: 11334831]

6. Patterson SWPH, Starling EH. The regulation of the ventricles. Journal of Physiology (Lond). 1914; 48:465–513. [PubMed: 16993269]
7. Crozatier B. Stretch-induced modifications of myocardial performance: from ventricular function to cellular and molecular mechanisms. Cardiovasc Res. 1996; 32:25–37. [PubMed: 8776400]
8. Allen DG, Kurihara S. The effects of muscle length on intracellular calcium transients in mammalian cardiac muscle. J Physiol. 1982; 327:79–94. [PubMed: 7120151]
9. White E, Le Guennec JY, Nigretto JM, Gannier F, Argibay JA, Garnier D. The effects of increasing cell length on auxotonic contractions; membrane potential and intracellular calcium transients in single guinea-pig ventricular myocytes. Exp Physiol. 1993; 78:65–78. [PubMed: 8448013]
10. Gautel M. Cytoskeletal protein kinases: titin and its relations in mechanosensing. Pflugers Arch. 2011; 462:119–134. [PubMed: 21416260]
11. Konhilas JP, Irving TC, de Tombe PP. Frank-Starling law of the heart and the cellular mechanisms of length-dependent activation. Pflugers Arch. 2002; 445:305–310. [PubMed: 12466931]
12. Izakov V, Katsnelson LB, Blyakhman FA, Markhasin VS, Shklyar TF. Cooperative effects due to calcium binding by troponin and their consequences for contraction and relaxation of cardiac muscle under various conditions of mechanical loading. Circ Res. 1991; 69:1171–1184. [PubMed: 1934350]
13. Moskvin AS, Philipiev MP, Solovyova OE, Kohl P, Markhasin VS. Electron-conformational model of ryanodine receptor lattice dynamics. Prog Biophys Mol Biol. 2006; 90:88–103. [PubMed: 16061275]
14. Li W, Kohl P, Trayanova N. Induction of ventricular arrhythmias following mechanical impact: a simulation study in 3D. J Mol Histol. 2004; 35:679–686. [PubMed: 15614623]
15. Lee S, Kim JC, Li Y, Son MJ, Woo SH. Fluid pressure modulates L-type Ca2+ channel via enhancement of Ca2+-induced Ca2+ release in rat ventricular myocytes. Am J Physiol Cell Physiol. 2008; 294:C966–976. [PubMed: 18272819]
16. Woo SH, Risius T, Morad M. Modulation of local Ca2+ release sites by rapid fluid puffing in rat atrial myocytes. Cell Calcium. 2007; 41:397–403. [PubMed: 17087992]
17. Belmonte S, Morad M. 'Pressure-flow'-triggered intracellular Ca2+ transients in rat cardiac myocytes: possible mechanisms and role of mitochondria. J Physiol. 2008; 586:1379–1397. [PubMed: 18187469]
18. Iribe G, Kohl P. Axial stretch enhances sarcoplasmic reticulum Ca2+ leak and cellular Ca2+ reuptake in guinea pig ventricular myocytes: experiments and models. Prog Biophys Mol Biol. 2008; 97:298–311. [PubMed: 18395247]
19. Iribe G, Ward CW, Camelliti P, Bollensdorff C, Mason F, Burton RA, Garny A, Morphew MK, Hoenger A, Lederer WJ, Kohl P. Axial stretch of rat single ventricular cardiomyocytes causes an acute and transient increase in Ca2+ spark rate. Circ Res. 2009; 104:787–795. [PubMed: 19197074]
20. Langton PD. Calcium channel currents recorded from isolated myocytes of rat basilar artery are stretch sensitive. J Physiol. 1993; 471:1–11. [PubMed: 8120799]
21. Farrugia G, Holm AN, Rich A, Sarr MG, Szurszewski JH, Rae JL. A mechanosensitive calcium channel in human intestinal smooth muscle cells. Gastroenterology. 1999; 117:900–905. [PubMed: 10500073]
22. Lyford GL, Strege PR, Shepard A, Ou Y, Ermilov L, Miller SM, Gibbons SJ, Rae JL, Szurszewski JH, Farrugia G. alpha(1C) (Ca(V)1.2) L-type calcium channel mediates mechanosensitive calcium regulation. Am J Physiol Cell Physiol. 2002; 283:C1001–1008. [PubMed: 12176756]
23. Amano S, Ishikawa T, Nakayama K. Facilitation of L-type Ca2+ currents by fluid flow in rabbit cerebral artery myocytes. J Pharmacol Sci. 2005; 98:425–429. [PubMed: 16079462]
24. Peng SQ, Hajela RK, Atchison WD. Fluid flow-induced increase in inward Ba2+ current expressed in HEK293 cells transiently transfected with human neuronal L-type Ca2+ channels. Brain Res. 2005; 1045:116–123. [PubMed: 15910769]
25. Park SW, Byun D, Bae YM, Choi BH, Park SH, Kim B, Cho SI. Effects of fluid flow on voltage-dependent calcium channels in rat vascular myocytes: fluid flow as a shear stress and a source of artifacts during patch-clamp studies. Biochem Biophys Res Commun. 2007; 358:1021–1027. [PubMed: 17524365]

26. Ding Y, Schwartz D, Posner P, Zhong J. Hypotonic swelling stimulates L-type Ca2+ channel activity in vascular smooth muscle cells through PKC. Am J Physiol Cell Physiol. 2004; 287:C413–421. [PubMed: 15070808]
27. Mitra R, Morad M. A uniform enzymatic method for dissociation of myocytes from hearts and stomachs of vertebrates. Am J Physiol. 1985; 249:H1056–1060. [PubMed: 2998207]
28. Cleemann L, Morad M. Role of Ca2+ channel in cardiac excitation-contraction coupling in the rat: evidence from Ca2+ transients and contraction. J Physiol. 1991; 432:283–312. [PubMed: 1653321]
29. Sham JS, Cleemann L, Morad M. Functional coupling of Ca2+ channels and ryanodine receptors in cardiac myocytes. Proc Natl Acad Sci U S A. 1995; 92:121–125. [PubMed: 7816800]
30. Birnbaumer L, Qin N, Olcese R, Tareilus E, Platano D, Costantin J, Stefani E. Structures and functions of calcium channel beta subunits. J Bioenerg Biomembr. 1998; 30:357–375. [PubMed: 9758332]
31. Wirtz HR, Dobbs LG. Calcium mobilization and exocytosis after one mechanical stretch of lung epithelial cells. Science. 1990; 250:1266–1269. [PubMed: 2173861]
32. Guharay F, Sachs F. Stretch-activated single ion channel currents in tissue-cultured embryonic chick skeletal muscle. J Physiol. 1984; 352:685–701. [PubMed: 6086918]
33. Sigurdson WJ, Sachs F, Diamond SL. Mechanical perturbation of cultured human endothelial cells causes rapid increases of intracellular calcium. Am J Physiol. 1993; 264:H1745–1752. [PubMed: 8322903]
34. Oike M, Droogmans G, Nilius B. Mechanosensitive Ca2+ transients in endothelial cells from human umbilical vein. Proceedings of the National Academy of Sciences of the United States of America. 1994; 91:2940–2944. [PubMed: 8159684]
35. Puro DG. Stretch-activated channels in human retinal Muller cells. Glia. 1991; 4:456–460. [PubMed: 1718863]
36. Ypey DL, Weidema AF, Hold KM, Van der Laarse A, Ravesloot JH, Van Der Plas A, Nijweide PJ. Voltage, calcium, and stretch activated ionic channels and intracellular calcium in bone cells. J Bone Miner Res. 1992; 7(Suppl 2):S377–387. [PubMed: 1283043]
37. Sharma RV, Chapleau MW, Hajduczok G, Wachtel RE, Waite LJ, Bhalla RC, Abboud FM. Mechanical stimulation increases intracellular calcium concentration in nodose sensory neurons. Neuroscience. 1995; 66:433–441. [PubMed: 7477884]
38. Nabauer M, Morad M. Ca2(+)-induced Ca2+ release as examined by photolysis of caged Ca2+ in single ventricular myocytes. Am J Physiol. 1990; 258:C189–193. [PubMed: 2301565]
39. Adachi-Akahane S, Cleemann L, Morad M. BAY K 8644 modifies Ca2+ cross signaling between DHP and ryanodine receptors in rat ventricular myocytes. Am J Physiol. 1999; 276:H1178–1189. [PubMed: 10199841]
40. Montero M, Alonso MT, Albillos A, Garcia-Sancho J, Alvarez J. Mitochondrial Ca(2+)-induced Ca(2+) release mediated by the Ca(2+) uniporter. Mol Biol Cell. 2001; 12:63–71. [PubMed: 11160823]
41. Goldhaber JI, Parker JM, Weiss JN. Mechanisms of excitation-contraction coupling failure during metabolic inhibition in guinea-pig ventricular myocytes. J Physiol. 1991; 443:371–386. [PubMed: 1822531]
42. Thule T, Ahn JR, Woo SH. Inhibition of L-type Ca2+ channel by mitochondrial Na+-Ca2+ exchange inhibitor CGP-37157 in rat atrial myocytes. Eur J Pharmacol. 2006; 552:15–19. [PubMed: 17054940]
43. Scott RH, Dolphin AC. Activation of a G protein promotes agonist responses to calcium channel ligands. Nature. 1987; 330:760–762. [PubMed: 2447504]
44. Hool LC. Hypoxia increases the sensitivity of the L-type Ca(2+) current to beta-adrenergic receptor stimulation via a C2 region-containing protein kinase C isoform. Circ Res. 2000; 87:1164–1171. [PubMed: 11110774]
45. Miriyala J, Nguyen T, Yue DT, Colecraft HM. Role of CaVbeta subunits, and lack of functional reserve in protein kinase A modulation of cardiac CaV1.2 channels. Circ Res. 2008; 102:e54–64. [PubMed: 18356540]

46. Zhou P, Zhao YT, Guo YB, Xu SM, Bai SH, Lakatta EG, Cheng H, Hao XM, Wang SQ. Beta-adrenergic signaling accelerates and synchronizes cardiac ryanodine receptor response to a single L-type Ca2+ channel. Proceedings of the National Academy of Sciences of the United States of America. 2009; 106:18028–18033. [PubMed: 19815510]
47. Wang W, Zhang H, Gao H, Kubo H, Berretta RM, Chen X, Houser SR. {beta}1-Adrenergic receptor activation induces mouse cardiac myocyte death through both L-type calcium channel-dependent and -independent pathways. Am J Physiol Heart Circ Physiol. 2010; 299:H322–331. [PubMed: 20495143]
48. Hermosilla T, Moreno C, Itfinca M, Altier C, Armisen R, Stutzin A, Zamponi GW, Varela D. L-type calcium channel beta subunit modulates angiotensin II responses in cardiomyocytes. Channels (Austin). 2011; 5:280–286. [PubMed: 21525790]
49. Shilkrut M, Yaniv G, Asleh R, Levy AP, Larisch S, Binah O. Tyrosine kinases inhibitors block Fas-mediated deleterious effects in normoxic and hypoxic ventricular myocytes. J Mol Cell Cardiol. 2003; 35:1229–1240. [PubMed: 14519433]
50. Bean BP, Nowycky MC, Tsien RW. Beta-adrenergic modulation of calcium channels in frog ventricular heart cells. Nature. 1984; 307:371–375. [PubMed: 6320002]
51. Kranias EG, Bers DM. Calcium and cardiomyopathies. Subcell Biochem. 2007; 45:523–537. [PubMed: 18193651]
52. Pinterova M, Liskova S, Dobesova Z, Behuliak M, Kunes J, Zicha J. Impaired control of L-type voltage-dependent calcium channels in experimental hypertension. Physiol Res. 2009; 58(Suppl 2):S43–54. [PubMed: 20131936]
53. Goonasekera SA, Hammer K, Auger-Messier M, Bodi I, Chen X, Zhang H, Reiken S, Elrod JW, Correll RN, York AJ, Sargent MA, Hofmann F, Moosmang S, Marks AR, Houser SR, Bers DM, Molkentin JD. Decreased cardiac L-type Ca(2)(+) channel activity induces hypertrophy and heart failure in mice. J Clin Invest. 2012; 122:280–290. [PubMed: 22133878]
54. Galli A, DeFelice LJ. Inactivation of L-type Ca channels in embryonic chick ventricle cells: dependence on the cytoskeletal agents colchicine and taxol. Biophys J. 1994; 67:2296–2304. [PubMed: 7696470]

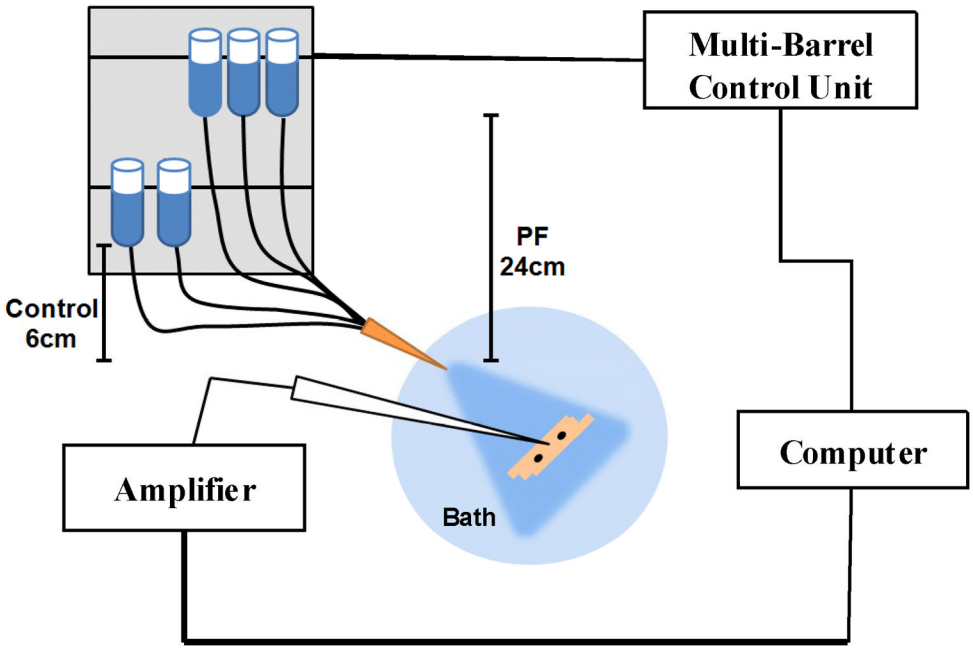

Figure 1. Schematic representation of the PF application

Solution barrels were kept at different levels, affording different gravity pressures that could be applied to cells by a PC controlled device. All the barrels converged to the same tip, avoiding differences in directions of solution being applied from different sides of the cell. Two levels of solutions were used, 6 cm and 24 cm.

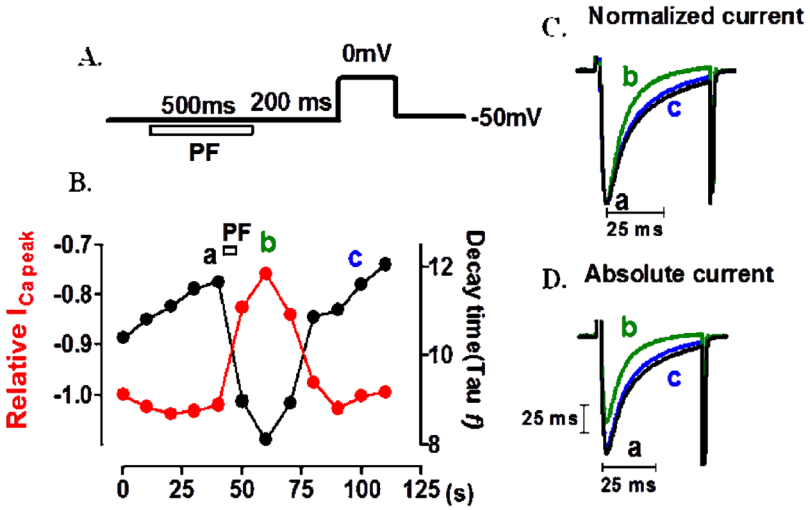

Figure 2. Effect of a brief PF in I_{Ca} dialized with 2mM EGTA

Depolarizing steps from −50mV to 0mV in cardiomyocytes causes calcium current activation (protocol in panel A), which is inactivated (black) and blocked (red) by a brief PF application (B). C. Sample trace or normalized current showing the change in inactivation kinetics in points a, b and c of Figure B. D. Sample trace or raw current showing the change peak amplitude in points a, b and c of Figure B. Internal solution used was a 2mM EGTA containing solution.

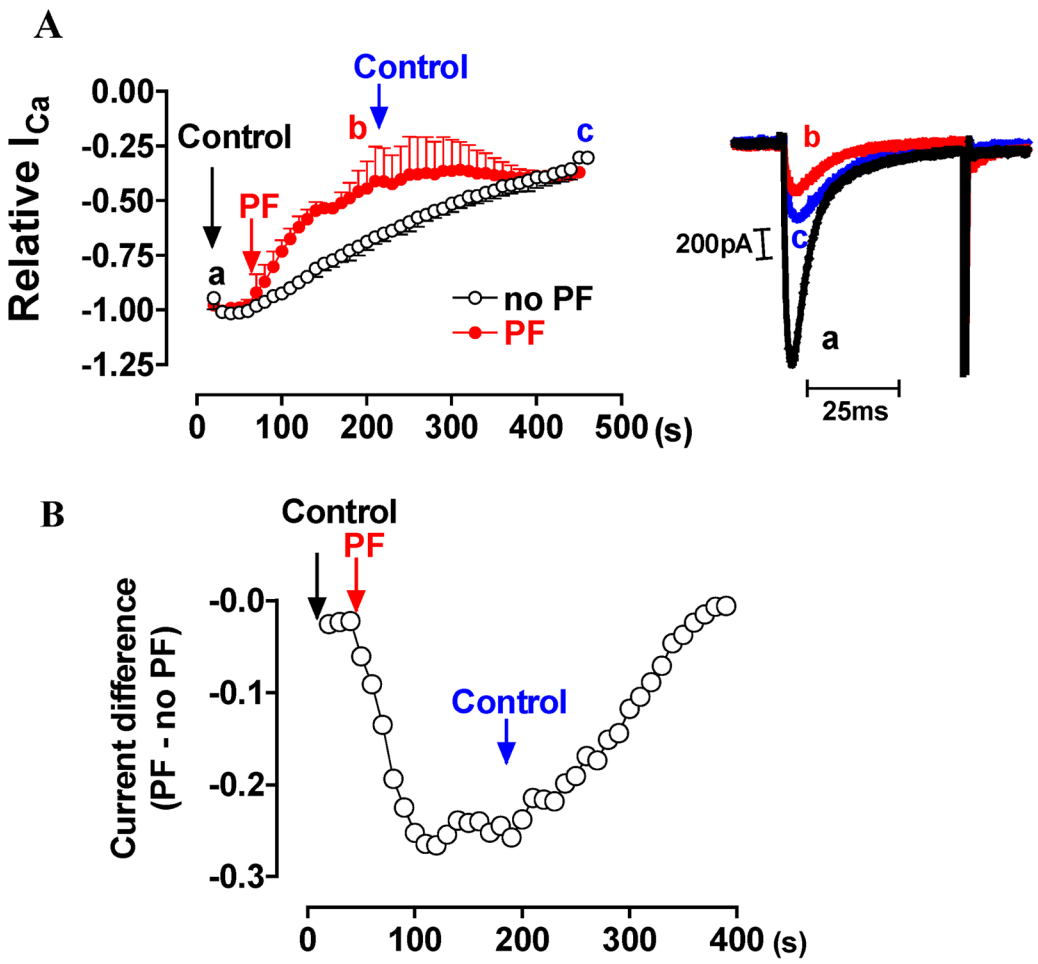

Figure 3. Effect of maintained PF in ICa

A.White circles represent control recordings from cells made in parallel, but not subjected to PF, recorded in the low flow bath all the time. Red circles represent the I_{Ca} of cell subjected to PF in the time indicated by PF. PF had the same compositions of bath solutions. Inset represent current before (a), during (b) and after continuous PF application (c). Data are mean ± SEM (n=3) B. Current difference between PF-and non PF-subjected myocytes. Internal solution used was a 0.2mM EGTA containing solution.

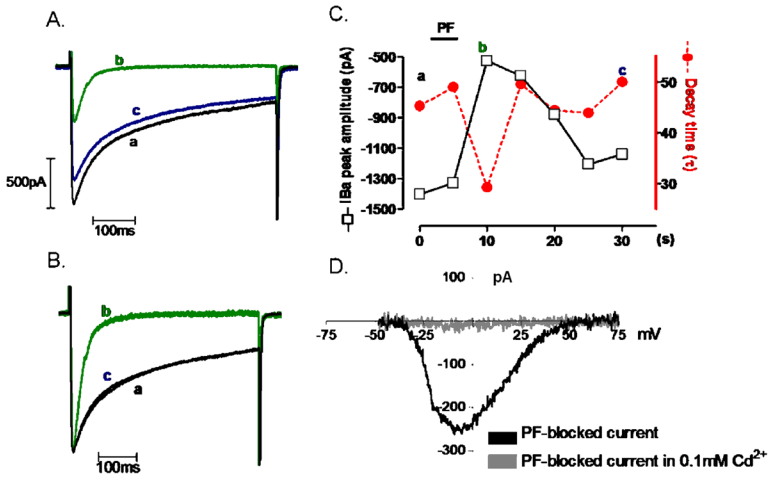

Figure 4. Pressurized-flow blocks L-type calcium channels and speeds their inactivation in cardiomyocytes

A) Effect of pressurized-flow in IBa amplitude (absolute current) and inactivation (normalized current) in cardiomyocytes before (a), 500ms after (b) or 15 seconds after a 500ms PF application (c). B) same traces are shown after normalization of peak current to put inactivation in evidence. C) Time course of peak suppression (black) and time constant of inactivation (red) during PF application. D) IV relationship of the current blocked by 500ms PF application in absence (black) or presence (grey) of Cd2+ using a ramp protocol from −50mV to +75mV evidencing calcium channels as PF target. Internal solution used was a 2mM EGTA containing solution.

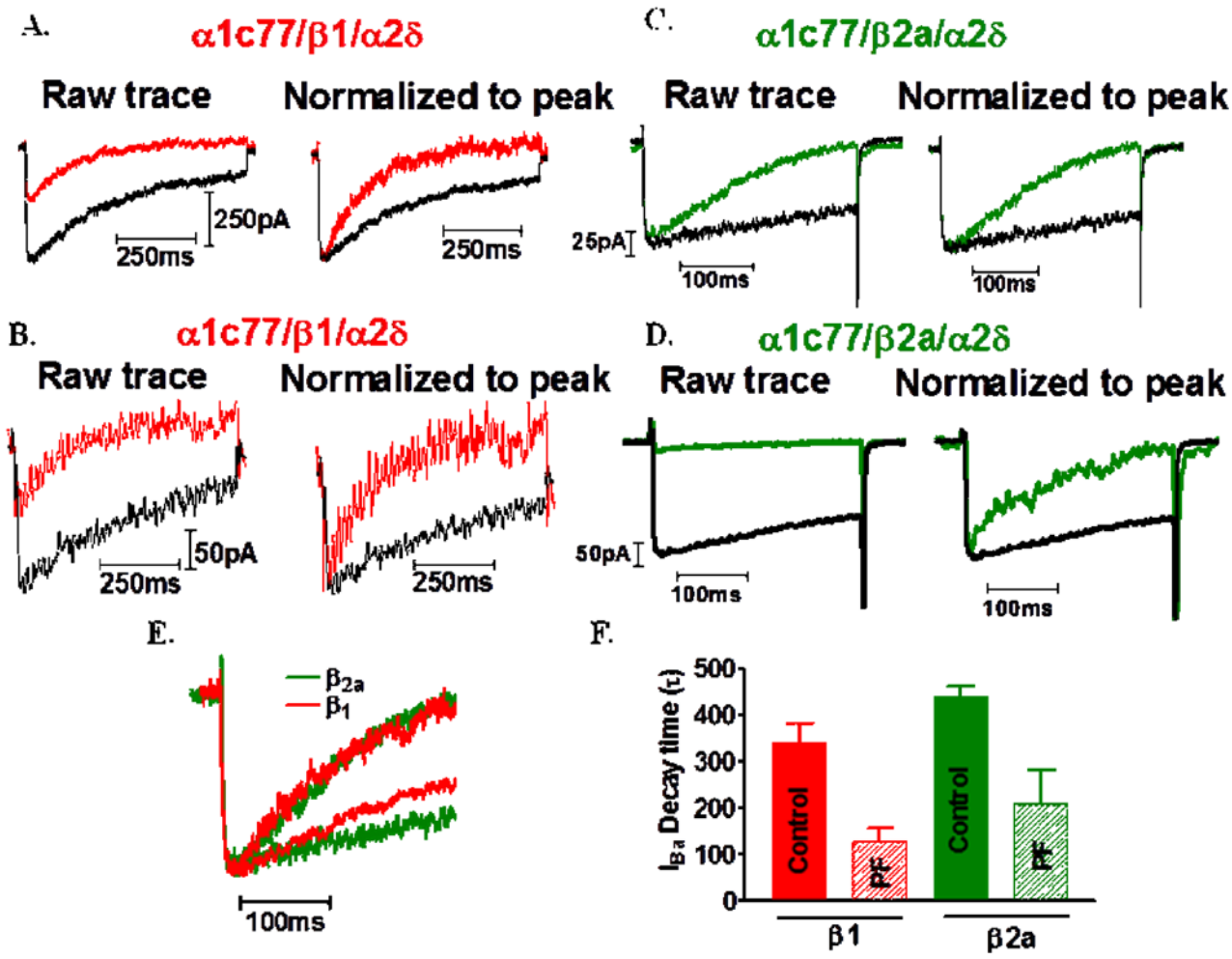

Figure 5. Pressurized-flow blocks α1c77/β1/α2δ and α1c77/β2a/α2δ human channels expressed in HEK 293 cells and speeds their inactivation

(A and B) Sample traces of I_{Ba} showing raw and normalized traces to evidence the effect of PF in peak amplitude and inactivation in α1c77/β1/α2δ channels. (C and D) Sample traces of I_{Ba} showing raw and normalized traces to evidence the effect of PF in peak amplitude and inactivation in α1c77/β;2a/α2δ channels . E. Superimposed sample traces of α1c77/β1/α2δand α1c77/β2a/α2δ channels showing a different inactivation kinetic at baseline conditions and an almost similar inactivation after PF stimulation. F. Quantification of PF effects in calcium channel time constant expressed in HEK cells. Data are mean ± SEM (n=3) Internal solution used was a 2mM EGTA containing solution.

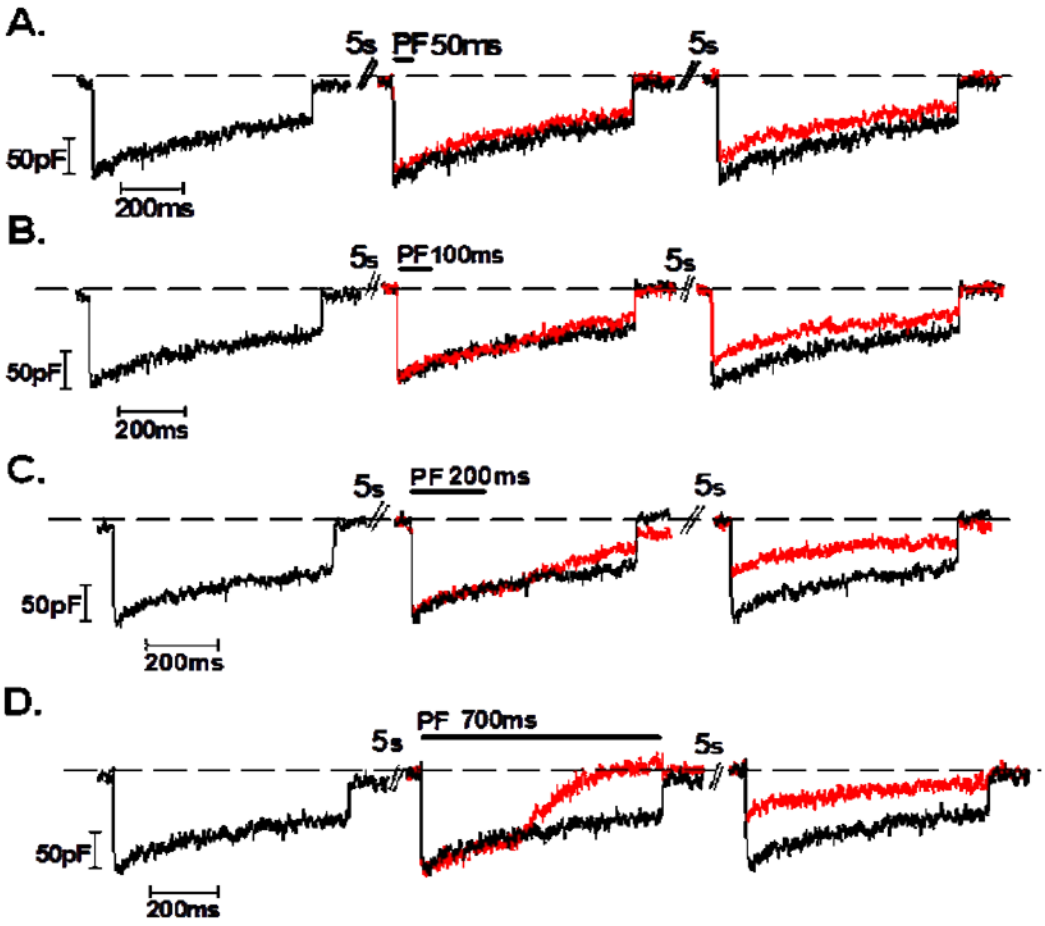

Figure 6. The duration of pressurized-flow determines the extent of blocking and inactivation of IBa through α1c77/β2a/α2δ channels expressed in HEK 293 cells

Control traces are shown in black, traces during and after 5s of PF application are shown in red. A. Effect of 50ms PF application in $I_{Ba.}$ current is barely blocked either immediately or after 5s of stimulation. B. Effect of 100ms PF application in $I_{Ba.}$ current is visible observed (middle trace in red)as a mild inactivation at the end of the trace which is enhanced during 5s interval and more evident in the following pulse. C. The effect of 200ms PF application in $I_{Ba.}$ current is observed (middle trace in red) as an inactivation at the end of the trace which is enhanced during 5s interval and more evident in the following pulse. 200. D. Effect of 700ms PF application in $I_{Ba.}$ current is observed (middle trace in red) as a strong inactivation from the middle to the end of the trace which is enhanced during 5s interval and still present in the following pulse. Internal solution used was a 2mM EGTA containing solution.

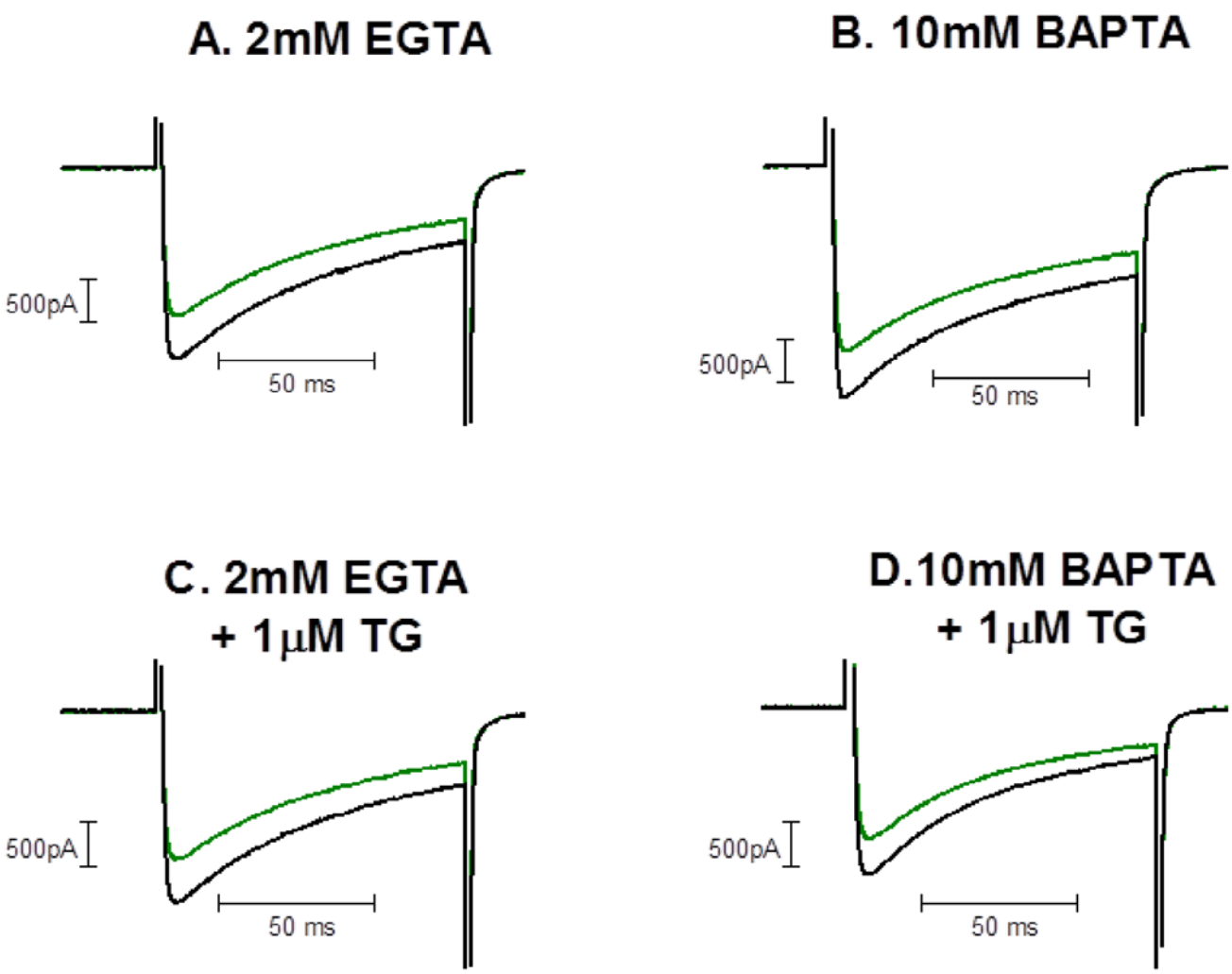

Figure 7. Effect of a brief PF in IBa in cells dialyzed with 2mM EGTA or 10mM BAPTA

Sample traces representing experimentsrepeated in 3 different days and three to four cells for each condition in each experimental day. Depolarizing steps from −50mV to 0mV in cardiomyocytes causes barium current activation, which is similarly suppressed by a brief PF application in control cells dialyzed with 2mM EGTA (A) or 10mM BAPTA (B); and in cells treated previously with 1mM of tapsigargin for 30min dialyzed with 2mM EGTA (C) or 10mM BAPTA (D). PF was applied for 500ms, followed by 500ms in control pressure solutions before depolarization for the test (PF) trace.

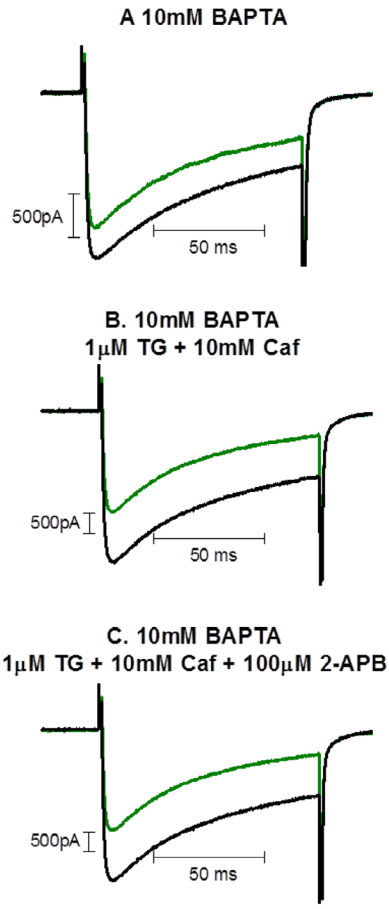

Figure 8. Effect of a brief PF in IBa in cells dialyzed with 10mM BAPTA, 10mM BAPTA plus 1mM tapsigargin or 10mM BAPTA plus 1mM tapsigargin and 10mM caffeine

Sample traces representing experiments repeated in 3 different days and three to four cells for each condition in each experimental day. Depolarizing steps from −50mV to 0mV in cardiomyocytes causes barium current activation, which is similarly suppressed by a brief PF application in cells treated previously with 1mM of tapsigargin and dialyzed with: (A) 10mM BAPTA; (B) BAPTA plus 1mM tapsigargin or (C) 10mM BAPTA plus 1mM tapsigargin and 10mM caffeine. PF was applied for 500ms, followed by 500ms in control pressure solutions before depolarization for the test (PF) trace.

Table 1

Effect of mechanical pressure on L-type calcium channels in different kind of cells and different subunit/splice variant expression

	Preparation	Channels	Internal solutions	External solutions	Effect observed	Stimulus
Langton, 1993 (Langton, 1993)	Rat basilar artery myocytes	$Ca_v1.2b$	CsCl 130, MgCl2 1, EGTA 5, ATPNa2 2, GTP 0.5, pH 7.2 or perforated patch	NaCl 130, KCl 5.4, glucose 10, BaCl2 10, EGTA 0.1, Hepes 10	Enhancement or suppression of peak amplitude	Pipette positive pressure (and hyposmotic sol.) or Pipette negative pressure (and hyperosmotic sol.)
Lyford et al., 2002 (Lyford *et al*., 2002)	HEK-293 or CHO cells	$Ca_v1.2b$ and $Ca_v1.2a$ − or + β2	Cs+ 145, 20 Cl−, EGTA 2, HEPES 5, 125 methanesulfonate	NaCl 149.2, KCl 4.7, 159 Cl −, 2.5CaCl2+, Hepes 5, 22ºC	Enhancement of current amplitude and faster inactivation, not mediated by C- terminal	Positive pressure or shear stress
Farrugia et al. 1999 (Farrugia *et al*., 1999)	Human Intestinal Smooth Muscle Cells	Native L- type calcium channels	Whole current (in mmol/L) Cs+ 145; Cl− 20, EGTA 2, HEPES 5, methanesulfonate 130 and single channels Ba+ 80, Cl − 160, HEPES 5	Whole cell Na+ 146,K+ 4.7, Cl− 154.7, Ca+2 2, HEPES 5 Single channels K+ 150; Cl− 154, Ca2+ 2, HEPES 5 pH ?	Increased peak current and open probability	Increased intracellular pressure and fluid pressure applied externally
Peng et al., 2005 (Peng *et al*., 2005)	HEK-293	$Ca_v1.2c$ + β3a + α2δ	CsCl 140, EGTA 10, HEPES 10 ATP-Mg 2, cAMP 1, pH 7.2, 2–25ºC	TEA-Cl 117, BaCl2 20, MgCl2 1, glucose 25, HEPES 10, TTX, 0.001, pH 7.2, ? ºC	Enhancement of current amplitude and faster inactivation	Shear stress
Lee et al., 2008 (Lee *et al*., 2008)	Ventricular Cardiomyocytes	Native channels ($Ca_v1.2a$ + β2+ α2δ)	CsCl 110, TEA- Cl 20, HEPES 20, MgATP 5, EGTA 2 (or BAPTA 10), pH 7.2	NaCl 137, KCl 5.4, HEPES 10, MgCl2 1, glucose 10, CaCl2 2(or BaCl2 2), pH 7.4, 2- 25ºC	Suppression of ICa but not IBa or ICa with BAPTA (0 Ca) internal	Localized fluid pressure
Amano et al. 2005 (Amano *et al*., 2005)	Rabbit Cerebral Artery Myocytes	Native channels	40 mM CsCl, 100 mM Cs aspartate, 10 mM TEA-Cl, 10 mM HEPES, pH 7.2, 270 μg/ml amphotericin B (perforated patch)	10 mM BaCl2, 50 mM NaCl, 10 mM TEA-Cl, 3 mM 4-AP, 5 mM HEPES, 5.5 mM glucose, 150 mM mannitol. pH 7.4	Enhancement of IBa	Hyperosmotic external solution
Park et al. 2007 (Park *et al*., 2007)	Rat superior mesenteric vascular myocytes	Native channels	nystatin 200 μg/ml, CsCl, 140 mM; MgCl2, 1 mM; Hepes, 5 mM; EGTA 0.05 mM; pH 7.2 (perforated patch)	143 mM NaCl, 5.4 mM KCl, 0.33 mM NaH2PO4, 10 mM BaCl2, 0.5 mM MgCl2, 5 mM Hepes, and 11 mM glucose, pH 7.4	IBa enhancement and inavtivation	Fluid pressure
Rosa et al., 2013 (present work)	Ventricular Cardiomyocytes and HEK-293	Native channels ($Ca_v1.2a$ + β2a+ 2δ), (α1c77 + β2a + α2δ) or (α1c77 + β1b+ α2δ)	CsCl 120, TEA- Cl 20, NaCl 5, HEPES 10, MgCl2 1, MgATP 5, EGTA 2 (or BAPTA 10), pH 7.2	NaCl 137, HEPES 10, MgCl2 1, glucose 10, CaCl2 2 (or BaCl2 2), pH 7.4, 2–25ºC	Suppression of ICa and IBa with EGTA or BAPTA (0 Ca^{2+}) internal	Localized pressurized fluid

Table 2

Effect of various inatracellular pathway blocker on PF-induced IBa block.

Compound	Mechanism	Effect
U73122 (1μM)	PLC inhibitor	↔
cAMP (200μM)	PKA activation	↔
Thapsgargin (1μM)	SERCA blocker	↔
Dinitrophenol (100μM)	Mitochondrial uncoupler	↔
FCCP (0.1–5μM)	Mitochondrial uncoupler	↔
Ru360 (5μM)	MCU blocker	↔
2-APB (100μM)	IP-3 receptor antagonist	↔
L-NAMME (1mM)	NOS inhibitor	↔
Pertussis toxin (0.1 μM)	G protein inhibitor	↔
BayK8644 (1μM)	Calcium channel agonist, CDI inhibitor	↔
CGP-37157 (1–10μM)	Mitochondrial NCX blocker	↔
Cyclosporin (500nM)	Inhibitor of cytochrome c release	↔
Caffeine (10mM)	Releases Ca^{2+} through RyR	↔
BAPTA (10mM)	Fast Ca^{2+} buffer	↔